Solar Energy 194 (2019) 804–814

Contents lists available at ScienceDirect

Solar Energy

journal homepage: www.elsevier.com/locate/solener

Flow through calorimeter to measure fluid heat capacity in CSP applications

Christoph Hilgert[a,*], Fabian Howar[b], Marc Röger[a]

[a] German Aerospace Center (DLR), Institute of Solar Research, PSA, Ctra. Senés Km. 4, P.O. Box 44, 04200 Tabernas, Almería, Spain
[b] RWTH Aachen University, Germany

ARTICLE INFO

Keywords:
CSP
Parabolic trough
Thermo-physical properties
Specific heat capacity
Heat transfer fluid
Thermal performance

ABSTRACT

Performance tests of concentrating solar collectors are based on energy balance studies which require accurate measurements of fluid mass flow rate, temperature difference over the collector length and the knowledge of the specific heat capacity of the used heat transfer fluid (HTF). Especially at operation temperatures in the range of 200–400 °C, the accuracy of HTF manufacturer data regarding the specific heat capacity of used HTFs is insufficient. This shortcoming contributes significantly to the overall measurement uncertainty of thermal collector assessments. In the present paper, the measurement results of a flow through calorimeter measuring the specific heat capacity of SYLTHERM 800 under field conditions at temperatures up to 330 °C are presented. The HTF measurement shows good agreement (deviation below 1.2%) with a Differential Scanning Calorimetry (DSC) measurement for temperatures below 270 °C. For higher temperatures, the deviation between flow through calorimeter and DSC measurement increases to 3.7% at 330 °C. Furthermore, several technical design and measurement improvements over the calorimeter design presented in 2012 are described in detail. A validation measurement using water reveals deviations below 0.1% from the water reference values at ambient temperatures. A stringent uncertainty analysis reveals the largest individual measurement uncertainty. The unexpectedly large uncertainty of the Coriolis mass flow sensors at temperatures above 270 °C is distinguished by a large individual uncertainty and the comparison to DSC.

1. Introduction

Concentrating solar power (CSP) technologies concentrate direct normal irradiation to generate heat. This heat can either be utilized directly or be converted into electricity by a thermodynamic cycle. Four different technologies are available usually referred to as, “parabolic dish”, “linear Fresnel”, “parabolic trough” and “central tower” (Fernandez, 2014). During the last decade, several commercial systems were installed word wide with a total number of 5.5 GWe by 2018 (HELIOSCSP, 2019). While parabolic dish and linear Fresnel technologies found fewer application, central tower and especially parabolic trough technology were widely used (NREL, 2019). Central tower receivers use, water/steam, molten salts or air as heat transfer fluid in order to transport the collected heat either to a thermal energy storage or directly to a thermodynamic cycle for power generation. Parabolic trough solar fields applying thermal oil as heat transfer fluid represent the majority of today’s CSP plants (NREL, 2019). Since the efficiency of the solar field plays a crucial role in the overall plant performance, accurate qualification methods characterizing the thermal performance of the collector systems are of high importance. For efficiency measurements, the thermo-physical properties of the HTF have to be known. The authors recognized large deviations between the manufacturer specifications and results from different laboratories which investigated the same fluid sample. Additionally, the manufacturer values do not account for any changes over time due to HTF degradation or aging (Barroso, 2012) in the installation. For this reason, the flow through calorimeter was developed to measure under typical operating conditions of a parabolic trough plant.

This paper describes the technical design, the validation measurements and results of a HTF measurement campaign of a flow through calorimeter bypass also referred to as KONTAS[1]-cp. This device is currently connected to the KONTAS test facility at Plataforma Solar de Almería (PSA). It is assembled in a rack which can easily be transported and connected to other facilities or commercial solar power plants.

The measurement of the specific heat capacity of fluids is commonly done by Differential Scanning Calorimetry (DSC) The alternative flow calorimeter approach to determine either reaction enthalpy or heat capacity is well-established. This concept is widely used in different scales (miniature (Taberner, 2015), large scale (Dauncey, 1978)), temperature ranges (low temp. (Handa, 1986), high temp. (Christensen,

* Corresponding author.
E-mail address: christoph.hilgert@dlr.de (C. Hilgert).
[1] **Kon**zentratorteststand **A**lmería **S**panien (Concentrator test rig Almería Spain)

https://doi.org/10.1016/j.solener.2019.11.029
Received 7 May 2019; Received in revised form 28 October 2019; Accepted 9 November 2019
Available online 14 November 2019

Nomenclature

ASTM	ASTM International, formerly known as American Society for Testing and Materials [–]
c	specific heat capacity [J/kgK]
CSP	concentrating solar power [–]
D	diameter [–]
DLR	Deutsches Zentrum für Luft- und Raumfahrt [–]
DSC	differential scanning calorimetry [–]
f	function
GUM	guide to the expression of uncertainties in measurement [–]
HCU	heating and cooling unit [–]
HTF	heat transfer fluid [–]
ITML	inlet temperature measurement location [–]
KONTAS	Konzentratorteststand Almería Spanien [–]
m	mass [kg]
N	number of inputs [–]
MP	measurement point [–]
MS	measurement section [–]
OTML	outlet temperature measurement location [–]
P	power [W]
Pt100	resistance thermometer made of platinum with 100 Ω at 0 °C [–]
PSA	Plataforma Solar de Almería [–]
$\dot{Q}$	heat flow [W]
u	uncertainty [–]
SCE	solar collecting elements [–]
T	temperature [°C]
Type A	uncertainty evaluation by the statistical analysis of a series of measurements [–]
Type B	uncertainty evaluation by manufacturer's specification, calibration certificates or experiences from former measurements [–]
t	time [s]
V	volume [m^3]
1/10 B	1/10 DIN class B
x	input estimate
Y	measurand

Greek symbols

Δ	difference
1σ or 2σ	coverage factor of 1 or 2

Subscripts

ap	approximated
c	combined
drift	drift related to retained or released heat
el	electric
i	input
ins	insulation
loss	related to heat loss to ambient
m	measured
ms	measurement section
ohm	resistive
p	isobaric
res	residence time
rod	rod (heater)

1986)) and at high pressures (Ernst, 1989). CSP related flow calorimeter applications are covered under state of the art.

The standard ASTM (2011) 1269E is a widely used method to determine the specific heat capacity by DSC. The determination is based on measuring and comparing the heat flow into the sample and the heat flow into a well-known reference material (sapphire). While solid material can be measured directly (no or open crucible), liquid materials must be contained in hermetic measurement crucibles, especially at temperatures above the boiling point. Thus, the preparation of the configuration of the sample in terms of: crucible type, filling degree, crucible firmness, sample mass, filling degree and crucible mass becomes important. This is true, especially for HTF measurement at temperatures leading to steam pressures at about 10 atmospheres. Literature values of the uncertainty of heat capacity measurements obtained by this method give a non-uniform picture (Rudtsch, 2002) due to a complex measurement method which it prone to errors for measurements of fluids at high pressures. An adapted method called modulated differential scanning calorimetry (MDSC) is used by Muñoz-Sánchez et al. (2017). Muñoz-Sánchez employs this method to determine the specific heat on molten salt-based nano fluids. The recognition of scattering results and associated uncertainties in the range of 2–20% from numerous authors in this field of application are reported. Several different factors are analyzed: crucible type, sample mass and moisture. However, the accuracy of heat capacity measurements for said HTF at relevant temperatures and pressures has not been sufficient so far.

This paper gives an overview over the state of the arte in heat capacity measurement in CSP, gives an detailed description of the setup of the presented calorimeter, shows the results of a validation measurement using water, presents the results of a field measurement with Syltherm 800 up to 330 °C, contains a detailed uncertainty analysis and closes with an outlook to further improve the presented measurement system.

2. State of the art – Heat capacity measurement in solar thermal applications

Most measurements are performed on small HTF samples which are characterized in a laboratory environment. Jung et al. (2014) perform Differential Scanning Calorimetry[2] SETARAM, 2014 to determine the heat capacity of HTFs (DOWTHERM A and SYLTHER 800) samples in mint and used conditions. The measurements are performed at temperature up to 400 °C. The reproducibility of these data was confirmed by multiple measurements. The combined measurement uncertainty amounts to 2% (no sigma reported). Gomez (2012) investigates the heat capacity of Therminol VP-1 from 300-370 °C with a DSC[3] following the standard ASTM E-1269-05. The combined systematic and random uncertainty of the heat capacity measurement of the average of 25 samples was determined to be ± 0.074 (3.09%) J/g K at 95% confidence (2σ). Segovia (2008) presents an automated flow calorimeter for the measurement of highly accurate isobaric heat capacities for pure compounds and mixtures in the range of −20 °C to 130 °C and 0.1-20 MPa. Measurement results for toluene and ethyl-1,1-dimethylethyl ether (ETBE) are presented. An estimated total (1σ) uncertainty below 0.5% is reported.

Two research groups have designed devices to measure the HTF heat capacity under operating conditions of a thermal loop (Collares-Pereira, 1981; Marchã, 2014; Hilgert, 2012). The first research group, Collares-Pereira et al. (1981) presents a calorimeter for solar thermal collector testing. The concept is taken up again by Marchã et al. (2014). A calorimeter prototype was built, calibrated with water as HTF and tested up to 180 °C using HTF. Measurement results show good accordance with HTF manufacturer values up to 160 °C, but a detailed

[2] "SENSYS evo TG-DSC" by Setaram - cylinder-type DSC – TN-149, Methode 3.1 (SETARAM, 2014).

[3] "DSC1 STARe" by Mettler-Toledo.

Table 1
Overview of technical improvements over the initial calorimeter design presented by Hilgert et al. (2012).

Finding	Countermeasure / Improvement	Section
Gas accumulation at measurement locations affecting the temperature reading of the Pt100 sensors	Installation of purge lines at both measurement location	Section 3.2 (Fig. 4)
Vibrations and plastic deformations affecting the temperature reading of the Pt100 sensors	Implementation of support tubes around sensors preventing vibrations, Mounting cutting rings before performing calibration measurements	Section 3.2 (Fig. 4)
Drifting and fluctuating mass flow during measurements	Using the mass flow sensor signal for a feedback control, actuating the control valve behind the measurement section compensating mas flow rate fluctuations	Section 5.1.3
Potential back flow of heated HTF in vertical pipe section below inlet temperature measurement location affecting the temperature reading	Introduction of an orifice behind the inlet temperature measurement location, preventing back flow / convection	Section 3.2 (Fig. 4)
Unintended loss of heated HTF leaving the measurements section towards the protection flow, affecting the energy balance	Hydraulic improvement of the "partition plate" by filling gaps with brazing solder and an additional circumferential sealing	Section 3.2 (Fig. 3)
Increased heat losses at temperatures above 70 °C	Recording the temperature dependent heat losses of the calorimeter	Section 4.2.1 (Fig. 9)

uncertainty analysis is not presented. The calorimeter measures the product $\dot{m}c_p$ which is the flow rate multiplied with the specific heat. Thus, an additional and accurate mass flow measurement is required to determine the specific heat capacity. The device has been calibrated using water as calibration medium. The second group formed by the authors, Hilgert et al. (2012), used a much larger device which also measures the mass flow rate, thus delivering specific heat capacity values. In contrast to (Collares-Pereira, 1981; Marchã, 2014), the device of Hilgert et al. does not need to be calibrated. This actual paper communicates results of recent water validation measurements, HTF measurements up to 330 °C and a detailed uncertainty analysis.

3. Setup of the flow through calorimeter

3.1. Improvements over the initial design

The flow through calorimeter design presented by Hilgert et al. (2012) was improved in several ways reacting upon findings and weak points detected during commissioning and test measurements. Said changes are listed below in Table 1 and are explained in the indicated sections.

3.2. Measurement concept of the flow through calorimeter

The specific heat capacity at a constant pressure and steady mass flow rate can be calculated as for a flow through setup according to

$$c_p = \frac{\dot{Q}}{\dot{m}\cdot(T_{\text{out}} - T_{\text{in}})}. \quad (1)$$

The general measuring principle for a flow through calorimeter is directly derived from this equation and leads to a basic measuring setup as shown in Fig. 1 (dashed box representing the energy balancing volume hereafter called measurement section (MS)). Hence, the calorimeter consists of a differential temperature measurement (for the measurement campaign a new set of Pt100 type 1/10B sensors is installed to the bypass), an electrical heater in combination with a wattmeter (Yokogawa WT 230) and a mass flow sensor (RHEONIK RHM 06 FHT – Transmitter RHE 08) to enable the heat capacity measurement. During measurements, a mass flow (rate measured by the flow meter) is heated by a heating device (rate measured by the wattmeter) and the resulting temperature rise is measured.

A detailed functional sectional view of the measurement setup is presented in Fig. 2. It shows both temperature measurement locations and the heater divided by the partition plate. The partition plate separates the measurement section where the active heater rods are located from the so called protection flow bathing the inactive heater rod sections. The protection flow feeds unavoidable and considerable heat losses at the heater flange which must not be insulated on its outer face. The rest of the setup is covered by amply dimensioned thermal insulation.

The partition plate separates two HTF flows of identical temperatures. Thus, it is a semi hermetic but adiabatic barrier which is penetrated by the inactive parts of the heater rods. The outer partition plate edge is sealed against the inner heater tube face in order to cope with lateral thermal expansion but restrict HTF cross flow. During measurements the pressure difference outside and inside the measurement section, across the partition plate, is adjusted in a way that a minor HTF flow from the protection flow side enters the MS thus, preventing a potential counter flow which could correlate to a heat loss from the MS.

The inlet temperature measurement location (ITML) and the outlet temperature measurement location (OTML) comprise identical geometries and setups apart from two details, see Fig. 4. At the ITML the flow direction is reversed and it is combined with an orifice in order to eliminated potential temperature increased backflow from the heater to the ITML. Both TML feature purge lines in order to periodical remove potential gas accumulations, static mixers to ensure a mean temperature measurement across the tube diameter, support tubes to prevent sensor vibration or deformation potentially caused by increased volume flows, a sensor immersion depth (15 D, 15 times the sensor diameter from its tip to the support tube) that excludes any conduction driven influence in the sensor readings and the option to execute relative calibration comparison measurements of all six sensors at one TML under identical and relevant flow conditions (see Section 5.1.1).

A secondary Coriolis sensor is integrated to measure the total mass flow rate through the attached facility usually being connected in line with the parabolic trough collector under investigation, see Fig. 1. This Coriolis sensor enables the recalibration of permanently installed mass flow sensors of the solar field instrumentation. Being connected to the KONTAS test bench, the flow through calorimeter is used to reduce the overall measurement uncertainty of efficiency tests performed there. The surrounding piping, sensors and data acquisition system are assembled in a separate add-on test rig depicted in Fig. 6. This DLR designed and built measurement bypass can accurately quantify the specific heat capacity of heat transfer fluids like Therminol VP1, SYLTHERM 800 or HELISOL® 5a under CSP relevant operating conditions. That means temperatures in the range of 20–350 °C[4] and pressure up to 18 bar. In terms of data acquisition, the device is designed for stand-alone operation. Thus, it operates independently from any plant

[4] This temperature is limited by the operation temperature of the Coriolis mass flow sensor.

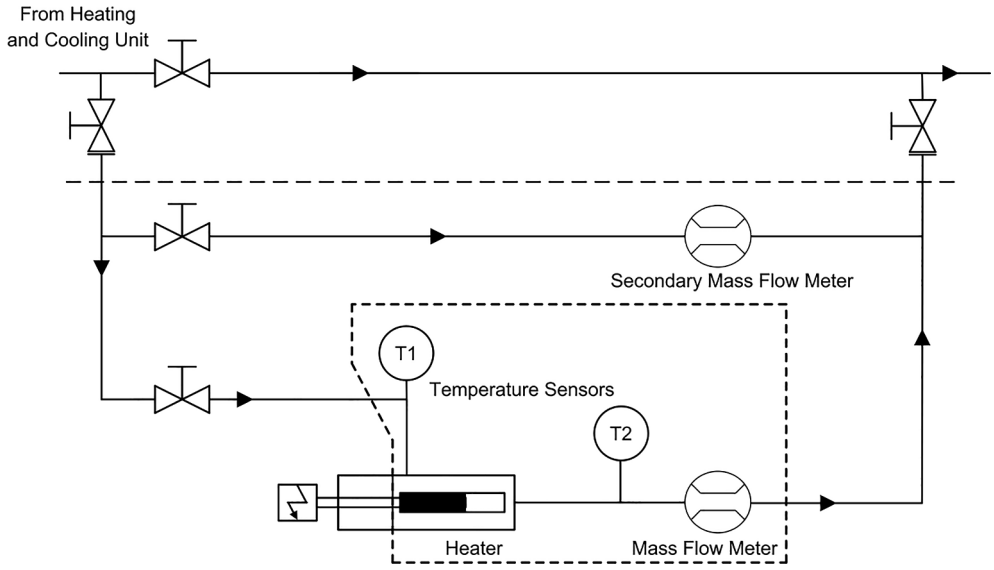

Fig. 1. Basic piping diagram of the flow through calorimeter setup indicating the measurement section (dashed box), the heater, the mass flow meter, the temperature measurement locations and the flow direction.

or facility data acquisition system. For this purpose, the bypass is connected to a laptop computer running a virtual instrument for system control and data acquisition. More details are presented by Hilgert et al. (2012). The flow through calorimeter device can be connected to an existing HTF circuit by two 2″ flange connections. For the measurement campaign presented in this paper, the bypass has been connected to the KONTAS facility, see Fig. 6.

Exact measurements require steady state conditions such as constant inlet and outlet temperatures, mass flow rate and heater power. To determine all influencing factors, which could possibly distort the measurement evaluation and results based on the ideal adiabatic and steady-state energy balancing approach, a series of considerations is made and described in this section. Measurements during heat-up or transient phases, with inconstant inlet temperatures or fluctuating mass flow rates require additional effort. Such measurements are not subject of this paper.

3.2.1. Residence time correction

The time a fluid particle needs to run through the measurement section of the bypass is the so-called residence time. The residence time

$$t_{res} = \frac{\rho V_{ms}}{\dot{m}}, \tag{2}$$

depends on the mass flow rate $\dot{m}$ and the density ρ of the analyzed fluid, while the enclosed volume of the measurement section V_{ms} is constant, assuming that influences by thermal expansion are negligible. A fluid particle entering the inlet temperature measurement location (ITML) at the time $t_0 - t_{res}$ with the temperature $T_{in}(t_0 - t_{res})$ is heated up in the measuring section and reaches the outlet temperature measurement location (OTML) at the time t_0. The interval between t_0 and $t_0 - t_{res}$ coincides with the residence time in which the temperature at the ITML changes to $T_{in}(t_0)$. The evaluation of the measurement data at the time $t_0 - t_{res}$ incorporates potential drifting of the inlet temperature (during the residence time) and leads to an decrease in the uncertainty of the measured temperature difference ΔT_m. The measured temperature difference is determined by

$$\Delta T_m = T_{out}(t_0) - T_{in}(t_0 - t_{res}) \tag{3}$$

The above represented approach answers to a streamline correction which uses the actual measured temperature at the time the considered fluid particle passed the ITML. Based on the calculated residence time, the evaluation at the time t_0 picks the inlet temperature from the recorded data vector at time $t_0 - t_{res}$. To measure the mass flow rate and temperature dependent residence time, a sudden temperature change is induced to the entering fluid. The entering temperature peak is detected at the ITML and later at the OTML as it travels through the measurement section. The difference in time is the residence time. During measurement evaluations t_{res} is calculated based on the known volume

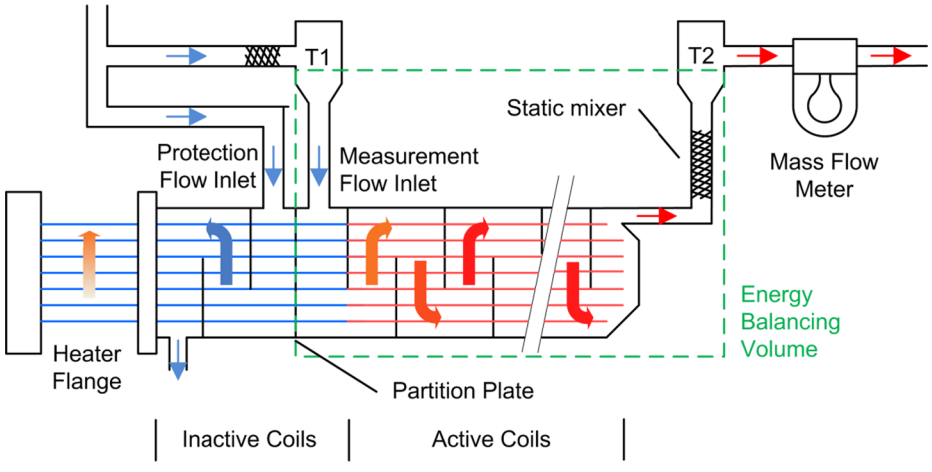

Fig. 2. Sectional view of the measurement setup, indicating:, the energy balance volume, flow directions, HTF temperatures (blue arrows - cold flow, red arrows – heated flow), the heater rods (blue line - inactive, red line – heated), the temperature measurements (T1, T2), the static mixers and the mass flow meter. (For interpretation of the references to colour in this figure legend, the reader is referred to the web version of this article.)

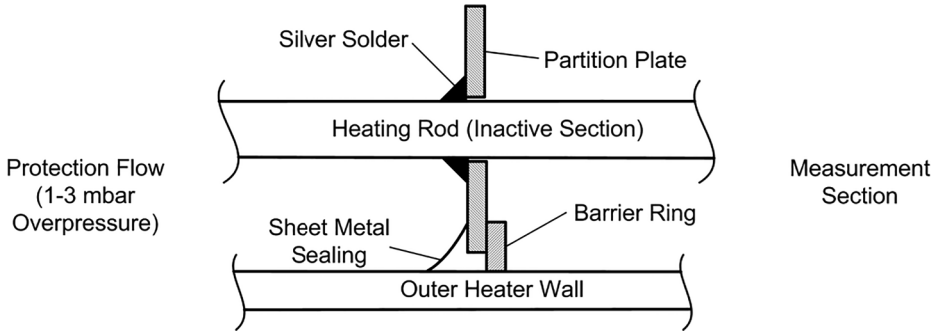

Fig. 3. Sectional view of the partition plate inside the heater indicating technical details.

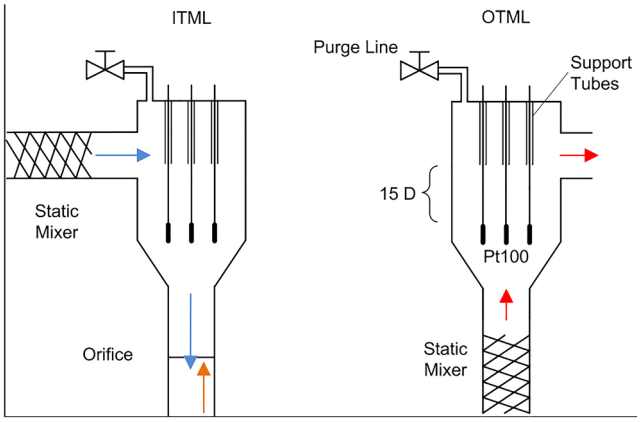

Fig. 4. Sectional view of the inlet (left) and the outlet (right) temperature measurement locations indicating the static mixers, the orifice, the purge lines, the sensor support tubes, the sensor immersion depth and the three redundant Pt100 temperature sensors.

of the measurement section, the fluid density (manufacturer table) and the measured mass flow rate according to Eq. (2).

3.2.2. Heat loss

The electrical power P_{el} measured with the power meter is not equal to the effective heat flow $\dot{Q}$ (Eq. (1)) provided to the HTF in the measurement section, as a number of losses are affecting the measurement method. The influences of temperature heater drift $\dot{Q}_{drift}$, ohmic heat loss $\dot{Q}_{ohm}$, and heat losses to the environment $\dot{Q}_{loss}$ are considered

$$\dot{Q} = P_{el} - \dot{Q}_{drift} - \dot{Q}_{ohm} - \dot{Q}_{loss}. \quad (4)$$

During heat-up phase, part of the introduced heat is absorbed by the measurement section warming up its components. Likewise, during cool-down phases, part of the heat is transferred from the components back to the fluid. Fluctuations in the inlet temperature either cause a heating or cooling of the components of the measurement section. This amount of retained or released heat $\dot{Q}_{drift}$ either leaving or entering the fluid inside the measurement section influences the measurement results. It is calculated as product of the measurement section's (excluding the contained HTF) heat capacity $c_{p,ms}$, its mass m_{ms} and its mean temperature gradient $\frac{\Delta T_{ms}}{\Delta t}$ according to

$$\dot{Q}_{drift} = c_{p,ms} m_{ms} (\Delta T_{ms}/t). \quad (5)$$

The power meter is connected by cables to the heating rods. Although being as short as possible, the ohmic loss $\dot{Q}_{ohm}$ in the connecting cables (R_{cable}) and also in the inactive part of the heater rods (R_{rod}) are approximated according to

$$\dot{Q}_{ohm} = 3(R_{rod} + R_{cable})I^2. \quad (6)$$

Finally, part of the heating power is lost from the measurement section to the environment by conduction through isolation materials ($\dot{Q}_{loss}$). Metallic supports inside the MS have been avoided to eliminate "heat bridges" or heat conductive connections. To determine the heat losses, several so-called blank measurements with switched off heater power are carried out in the relevant temperature interval between 50 and 350 °C, see Fig. 9 (Heat Loss Measurement).

3.3. Validation measurement setup with water

For testing and validation purposes the flow through calorimeter was connected to a water circuit. A corresponding flow scheme is shown in Fig. 5. A circulation pump provides the flow through calorimeter with de-mineralized water from a reservoir.

Heat capacity measurements with water were performed in order to validate the functionality of the flow through calorimeter. As in the unpressurized water circuit no tempering was provided, the fluid leaving the tank had ambient temperature of about 20 °C at the beginning of the measurement. Throughout the measurement it was slowly heated up to about 50 °C by means of the electric heater used for the measurement.

3.4. Measurement setup with HTF at the KONTAS facility

The KONTAS rotary test bench is installed at Plataforma Solar de Almería (PSA) and enables thermal and optical performance measurements of parabolic trough modules (Solar Collecting Elements, SCE) and their components up to 20 m module length (Heller, 2011). KONTAS consists of a rotating base frame with a platform carrying a heating and cooling unit (HCU) and the exchangeable SCE to be examined. Azimuth and elevation drives allow for a module tracking at any desired angle of incidence of the solar radiation. A pump integrated in the HCU realizes the circulation of the HTF (SYLTHERM 800) through the collector module/receiver tubes. The HCU is designed to provide a steady circulation of the HTF up to a maximum mass flow rate of 6 kg/s at any desired temperature between ~40 and 400 °C. This represents thermo-hydraulic operation conditions very similar to commercial plant applications. The KONTAS measurement concept aims at a total accuracy of 2–3% for thermal performance tests on SCEs. These numbers are based on the current KONTAS measurement equipment and on the specific heat capacity measurement with an uncertainty of

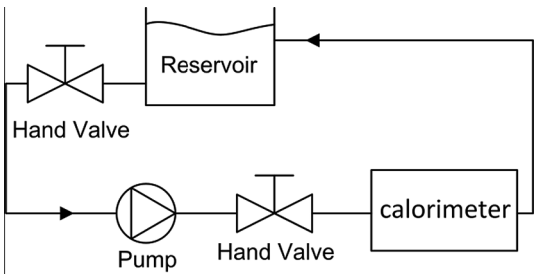

Fig. 5. Basic piping diagram of the water validation measurement setup.

Fig. 6. KONTAS-cp flow through calorimeter installed at KONTAS facility.

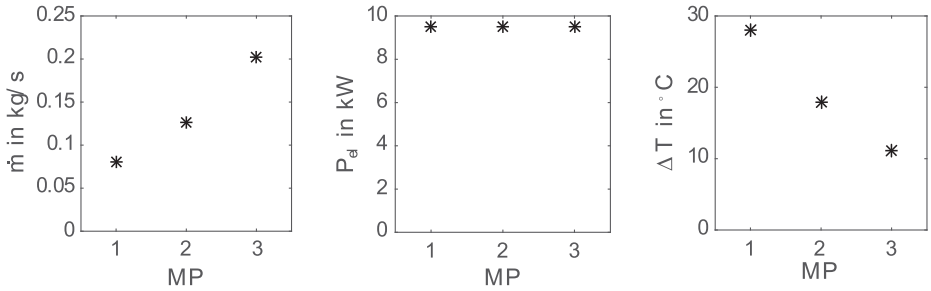

Fig. 7. Mass flow rate, electrical power and temperature difference at 3 measurement points (MP), inlet temperatures at MP1 36 °C, MP2 36 °C and MP3 38 °C.

1% valid for temperatures up to 260 °C. Fig. 6 shows the flow through calorimeter connected to the KONTAS test facility at PSA.

The hydraulic measurement setup is illustrated in Fig. 1. The heating and cooling unit directly feeds the conditioned HTF in terms of temperature and mass flow to the inlet of the calorimeter where the flow optionally passes through the device or bypasses it.

4. Measurement and results

4.1. Validation measurement with water

To study the influences of mass flow rate and temperature difference in the measurement result, three different measurement points (MPs) were adjusted. As shown in Fig. 7 the mass flow is gradually increased over the three MPs, while the electrical power is held constant.

As expected, the measured temperature difference between in- and outlet decreased inversely proportional to the mass flow rate. The results of the measurement are plotted in Fig. 8 complemented with the reference values, taken from IAPWS (2007). The reference values are denoted with an uncertainty of 0.2%. The measurement results of the specific heat capacity do not deviate more than 0.07% from the reference values. Although the result of MP3 still matches the reference value very well, the calculated[5] relative overall uncertainty increases (red uncertainty bar). This is a result of a rising absolute uncertainty of the temperature difference measurement $u_{\Delta T}$, as the values of ΔT over the measurement section decrease from around 30–10 K, while the temperature measurement accuracy is set to a constant value of 0.1 K based on relative calibration results.

The validation measurement results at about 36 °C using demineralized water prove the functionality of the calorimeter at ambient temperatures and low pressures. The deviation of less than 0.1% from the IAPWS (2007) reference values illustrates the highly accurate reading of the flow through calorimeter device under said conditions. Furthermore, the results of the validation measurement represent the effectiveness of the technical design and measurement improvements introduced (See Sections 3.1 and 5.1). While in 2012 (Hilgert, 2012) fluctuating deviations between 0.12% and 2.0% were found, the more recent results do not deviate more than 0.1% from the reference.

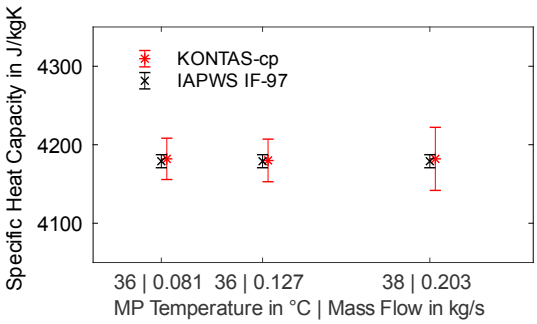

Fig. 8. Results of three heat capacity validation measurements using water (red stars) in comparison to the reference values (black cross) (lateral shift for improved legibility). (For interpretation of the references to colour in this figure legend, the reader is referred to the web version of this article.)

[5] At this temperature level a valid calibration certificate for the Coriolis sensor is incorporated.

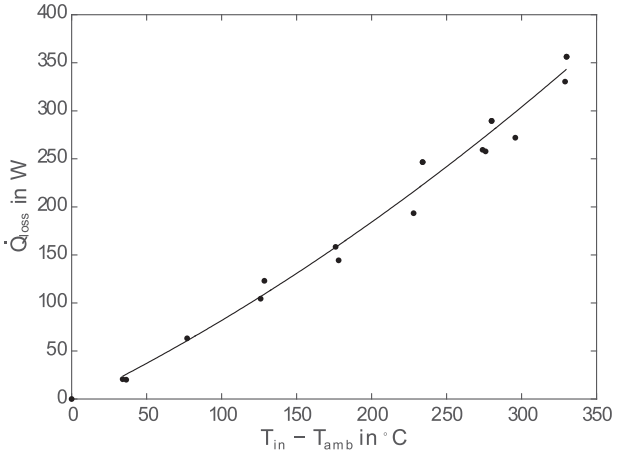

Fig. 9. Correlation of heat loss from the measurement section to the environment, based on several measurements (dots) at different HTF inlet temperatures and ambient conditions.

4.2. Measurement with SYLTHERM 800 at up to 330 °C

4.2.1. Heat loss measurement

While the heat losses ($\dot{Q}_{loss}$) during validation measurements near ambient temperatures have little to no influence on the measurement, they cannot be neglected for the HTF measurements at higher temperatures. Several blank measurements at different HTF temperatures with deactivated heater are executed to determine the temperature decrease over the measurement section ΔT_{loss} caused by $\dot{Q}_{loss}$. Thus, the inlet temperature of the measurement section is adjusted and maintained at the defined MP mean temperature by means of the HCU. After a heat up phase and completion of thermal equilibration, a steady-state temperature drop ΔT_{loss} is measured across the measurement section. Since the entire setup is well insulated, especially at low HTF temperatures a measurable ΔT_{loss} occurs only at relatively low flow rates. Still, a minimum flow rate must be respected in order to ensure a homogeneous temperature profile inside the heater and the connected tubes. The results of several heat loss measurements respecting a minimum mass flow of 120 g/s are plotted in Fig. 9. These values are calculated according to Eq. (7) using the approximated heat capacity ($c_{p,ap}$) based on DSC measurements (Fig. 12). The heat losses increase with the difference between inlet and ambient temperature and are as high as 350 W at 330 °C. For each c_p measurement, a blank measurement is done directly before the heat capacity measurement and the corresponding temperature drop ΔT_{loss} is used in

$$\dot{Q}_{loss} = \dot{m} \cdot c_{p,ap} \cdot \Delta T_{loss}. \tag{7}$$

4.2.2. HTF heat capacity measurement

Due to the thickness of the thermal insulation layer of approximately 20 cm and considerable steel mass m_{ms} (app. 62 kg) of the measurement section, thermal equilibration is reached about 2.5 h after first measuring the set inlet temperature. Once the thermal equilibrium is reached, the blank measurement can be executed. Subsequent to the blank measurement, the inlet temperature is lowered by half of the expected temperature rise caused by the heater power, to adjust the mean temperature of the measurement section to the measurement point mean temperature. After app. 15 min, thermal equilibrium and thereby measurement readiness is reached. The temperature profiles of this procedure are plotted in Fig. 10.

Based on Eq. (1) considering Eqs. (4)–(6) the specific heat capacity is written as

$$c_p = \frac{P_{el} - \dot{Q}_{drift} - \dot{Q}_{ohm}}{\dot{m}(\Delta T_m - \Delta T_{loss})}. \tag{8}$$

Fig. 11 and Table 2 provide an overview over the measurands at each MP. For the heat capacity measurements the mass flow is adjusted to 0.219 kg/s while the heater control is set to full load. Nevertheless, decreasing heater power P_{el} is measured, which originates from the temperature dependent heater performance characteristic (see Fig. 11, top right). The decrease of the temperature difference is not only caused by the declining heater power, but is also influenced by the increasing specific heat capacity of SYLTHERM 800 at higher temperatures.

Manufacturer's data of the HTF properties rely on a clean and unused fluid and thereby do not necessarily represent a useful reference for operation related c_p measurements. To obtain a more precise and reliable reference of the same fluid, a sample of the very same oil utilized in KONTAS was taken and sent to the laboratory of the Institute of Solar Research in Cologne to examine the specific heat capacity by the DSC presented by Jung et al. (2014). The results of the specific heat capacity measurements from the flow through calorimeter of April 2016 are presented in Fig. 12 and Table 2 in comparison to manufacturer's data and reference values from the DSC, measured in 2014 and 2017[6] both taken from the identical HTF filling at the facility.

The heat capacity data given by the manufacturer is in average 2.5% lower than the DSC results and 3.8% lower than the values measured with KONTAS-cp. Since the manufacturer guarantees an uncertainty of the specified heat capacities of below 10%, such relative deviations are within the domain of uncertainty. It can be assumed that the intersection of the three uncertainty domains (DSC, KONTAS-cp and manufacturer) gives a suitable approximation of the true value.

Particularly in the lower and middle temperature range between 160 °C and 270 °C, DSC and KONTAS-cp results nearly coincide. The observed deviation is 0.5% for temperatures below 210 °C and increases to 1.2% at 269 °C. Above this value, the deviation grows significantly with an increasing measurement temperature reaching up to 3.7% for the measurement at 329 °C, see Table 3.

DSC results are denoted with an uncertainty of 2% (1σ), whereas manufacturer guarantees only < 10%. The measurement uncertainty of the flow through calorimeter device is analyzed in the following section.

5. Uncertainty analysis

The uncertainty analysis follows the "Guide to the Expression of Uncertainties in Measurement" (GUM) (JCGM, 2008). Two evaluation methods Type A (evaluation by the statistical analysis of a series of measurements) and Type B (evaluation by manufacturer's specification, calibration certificates or experiences from former measurements) are determined individually and thereupon the combined uncertainty u_c of the specific heat capacity measurement is calculated according to

$$u_c(Y) = \sqrt{\sum_{i=1}^{N} \left(\frac{\partial f}{\partial x_i}\right)^2 u^2(x_i)}. \tag{9}$$

The function f is given in Eq. (8). Based on the data presented in Tables 2 and 4 the combined two sigma uncertainty is calculated according to

$$c_p = \frac{P_{el} - \dot{Q}_{drift} - \dot{Q}_{ohm}}{\dot{m}(\Delta T_m - \Delta T_{loss})}. \tag{10}$$

The uncertainty of the residence time affects the temperature difference measurement. The residence time based correction of the temperature difference measurement depends on the quality of the residence time determination in combination with the gradient of a potential temperature drift. While the temperature drift is typically

[6] In the meantime KONTAS was operated somewhat less than 1000 h at 350 °C or below, thus the occurrence of significant HTF degradation is very unlikely.

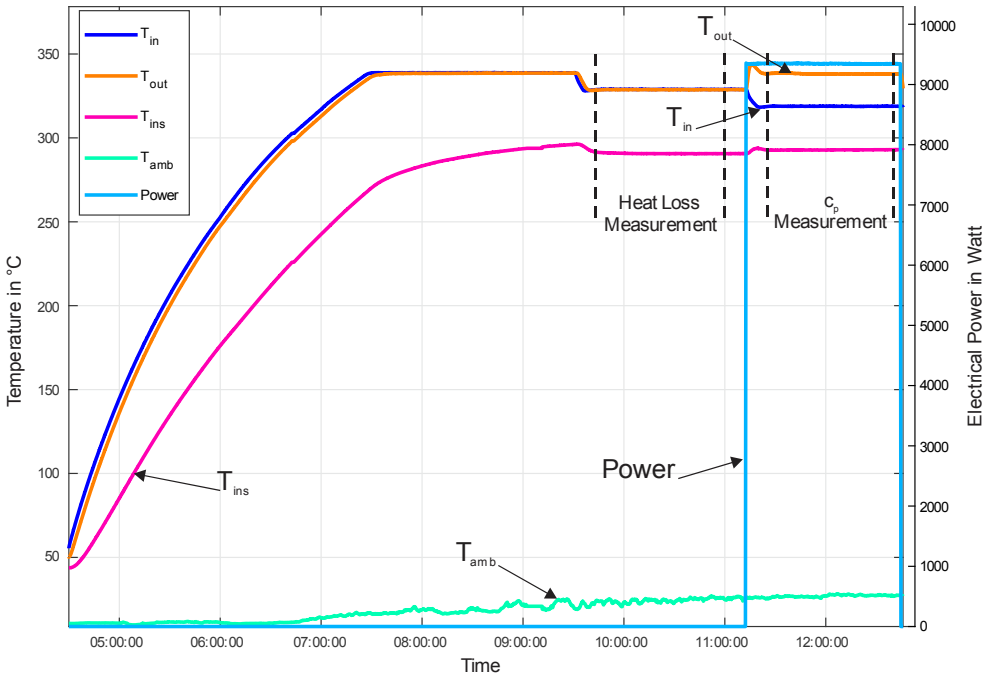

Fig. 10. Warming-up curves and stationary periods for flow through calorimeter heat loss determination and c_p measurement for inlet and outlet temperature (T_{in}, T_{out}), insulation and ambient temperature (T_{ins}, T_{amb}) and heating power of flow through calorimeter.

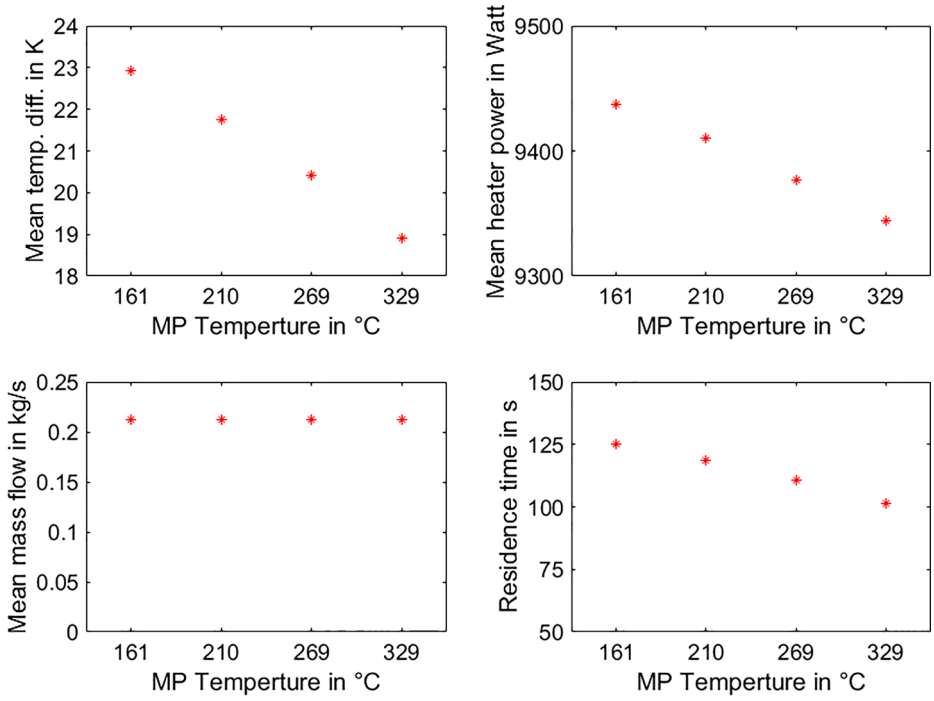

Fig. 11. Mean temperature difference between inlet and outlet (top left), mean heater power (top right), mean mass flow (bottom right) and residence time (bottom left) for four different mean temperatures (measurement points MP) to determine the specific heat capacity.

smaller than 0.001 K/s the residence time can be determined with an accuracy of 5 s. Thus, the worst case uncertainty in the temperature difference measurement is 0.005 K and hence neglected.

The resulting relative uncertainty contributions are plotted in Fig. 13 for each MP.

5.1. Type B uncertainties

5.1.1. Differential temperature measurement

All six Pt100 type 1/10B are equipped with cutting rings before calibration as plastic deformations of the sensor tubes may cause systematic uncertainties in the sensor reading. Subsequently, the sensors

Table 2
Magnitudes of quantities as measured during the four heat capacity measurements, the value in parenthesis is the ratio of the respective heat flow and P_{el}.

MP temp. in °C	P_{el} in W	$\dot{Q}_{loss}$ in W	$\dot{Q}_{drift}$ in W	$\dot{Q}_{ohm}$ in W	ΔT_{loss} in K	t_{res} in s
161	9438 (100%)	125 (1.33%)	−1.0 (−0.01%)	12.2 (0.13%)	0.31	125
210	9410 (100%)	169 (1.80%)	5.2 (0.05%)	12.1 (0.13%)	0.40	119
269	9377 (100%)	223 (2.38%)	−10 (−0.11%)	12.1 (0.13%)	0.50	111
329	9344 (100%)	277 (2.96%)	0.0 (0.0%)	12.0 (0.13%)	0.60	101

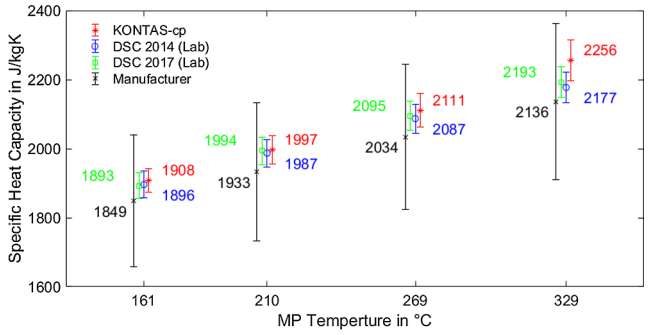

Fig. 12. Comparison of heat capacity measurement results with uncertainty bars over HTF temperature at 161 °C, 210 °C, 269 °C and 329 °C for the flow through calorimeter (KONTAS-cp), DSC laboratory measurements and manufacturer data (lateral shift for improved legibility).

Table 3
SYLTHERM 800 heat capacity measurement results and deviations between flow through calorimeter (KONTAS-cp), both laboratory DSC measurements and manufacturer data (DOW, 1997).

MP Temp in °C	KONTAS-cp in J/kgK	DSC (Lab) 2014 in J/kgK	DSC (Lab) 2017 in J/kgK	$\frac{Kontas_{cp} - DSC(2014)}{DSC}$ in %	Man. Data in J/kgK	$\frac{Kontas_{cp} - Man.Data}{Man.Data}$ in %
161	1903	1898	1887	0.5	1848	3.2
210	1993	1987	1998	0.5	1932	3.4
269	2106	2086	2092	1.2	2032	3.9
329	2247	2174	2188	3.7	2132	5.8

Table 4
Type B uncertainties based on manufacturer specified uncertainties and test measurements at DLR.

Quantity	Symbol	Uncertainty
Electrical power	P_{el}	0.1% of reading + 0.1% of range
Heater temperature drift[a]	$\dot{Q}_{drift}$	1 W
Residence time	t_{res}	neglected
Electrical heat loss[a]	$\dot{Q}_{ohm}$	1 W
Heat loss[a]	ΔT_{loss}	0.1 K
Temperature difference[a]	ΔT_m	0.1 K
Mass flow rate[b]	$\dot{m}$	0.6% of the reading + 0.005%/°C

[a] Estimated uncertainty by DLR based on external sensor calibrations and test measurements.

[b] For T < 90 °C; $\dot{m}$ = [0.021; 0.330] kg/s: < 0.2% of reading (RHEONIK Coriolis manufacturer) after re-calibration) for T > 90 °C: not specified nor guaranteed by Coriolis manufacturer; estimation based on empiric observation, see also Section 5.

are calibrated absolutely in a block calibrator[7]. In a next step all six sensors are mounted in the outlet temperature measurement location (see Fig. 4) in order to enable a relative calibration at relevant flow conditions using identical data acquisition hardware, thus compensating possible influences by the data acquisition hardware. Intentional purging at both measurement locations makes sure no accumulated air bubbles are interfering with the temperature measurement. After executing this procedure, the two sigma uncertainty of the temperature difference measurement including temperature transmitters is estimated to be less than 0.1 K.

5.1.2. Power measurement

The power transfer to the heater and homogeneity of the conversion to heat are cross checked individually by thermography. The manufacturer specifies an uncertainty of the power meter of ± 20 W at 10 kW reading, see Table 4. This uncertainty was reviewed by comparing the reading of the digital power meter[8] to a recently calibrated and more precise power meter from a different manufacturer (LMG 450 by ZES ZIMMER Electronic Systems GmbH; uncertainty of ± 6.6 W absolute at 9500 W reading). Furthermore the heat loss due to electrical resistance of the conductor between watt meter and heater was examined. During measurements this loss is subtracted from the power reading. Grid fluctuations affecting the heating power were compensated by means of an uninterrupted power supply.

5.1.3. Mass flow measurement

The mass flow through the measurement section is determined by means of a Coriolis mass flow sensor. A mass flow regulation has been integrated making use of the Coriolis mass flow sensor reading fed to a PID controller manipulating an automatic valve which regulates the mass flow through the measurements section. This mass flow regulation maintains the flow with a single standard deviation of 0.00014 kg/s (0.11% of reading) to the desired set value.

According to manufacturer's specification[9] the uncertainty in the interval between 0.021 kg/s and 0.33 kg/s should be smaller than 0.2% of the reading. During commissioning of flow through calorimeter the accuracy of the mass flow sensor was reconsidered. Due to the determination of systematic deviation, the sensor was sent to SP Technical Research Institute of Sweden for recalibration revealing significant measuring uncertainties (> 1%) even at ambient temperatures. A recalibration was performed at +20 °C and at 90 °C to detect possible temperature dependencies. The denoted uncertainty however is only valid at the calibration temperature even though the sensor is designed for temperatures up to 350 °C. Taking these results into account, a significantly larger and temperature depended uncertainty is considered for measurement evaluation at temperatures higher than 90 °C, see Table 4. As the information basis regarding this issue is insufficient both in literature as from side of the manufacturers of Coriolis sensors, this uncertainty at temperatures higher than 90 °C is not scientifically based, but a mere assumption based on empiric observations.

[7] AMETEK RTC-700 B with STS-200A 970 and DLC-700.

[8] Yokogawa WT 230.

[9] RHEONIK RHM 06 FHT – Transmitter RHE 08.

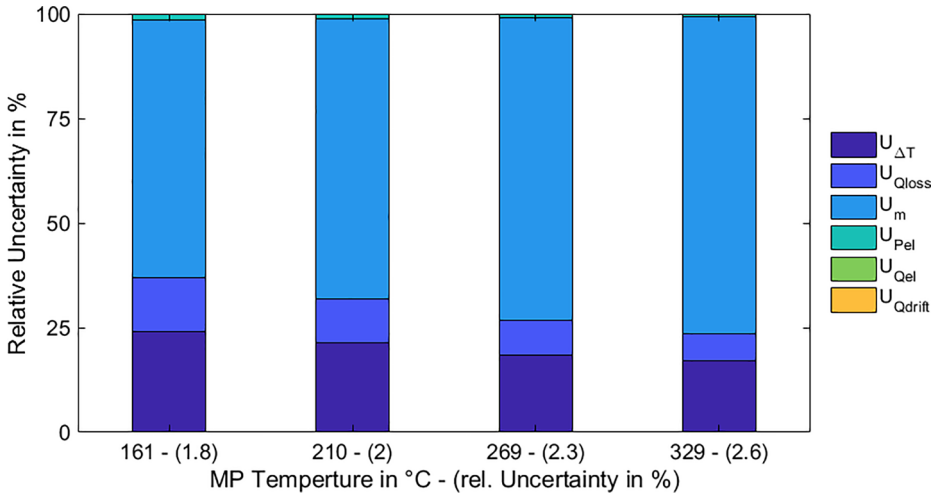

Fig. 13. Relative uncertainty contributions of individual measurands over measurement points (MP), combined relative uncertainty denoted in parentheses.

6. Outlook

For future measurements, the issue of increased mass flow rate uncertainties in relevant temperature ranges over 260 °C must be solved, either by a more suitable Coriolis sensor temperature correction or by reducing the Coriolis sensor operation temperature. The former approach implies remarkable technical calibration effort at elevated temperatures and is unlikely to be available in near future. Thus, the second approach operating the Coriolis sensor at temperatures e.g. below 200 °C is the only realistic option. A technical approach making use of an additional heat exchanger and an air cooler is presented in Fig. 14. The HTF flowing towards the Coriolis mass flow sensor is cooled by means of a plate and shell heat exchanger which transfers the heat to the flow upstream the Coriolis sensor. The additional air cooler serves to precisely regulate the temperature of the Coriolis sensor.

7. Conclusion

Specific heat capacity measurements were performed with the flow through calorimeter at a water circuit and at the KONTAS facility, which proved the functionality of the calorimeter at ambient temperatures using water and at temperatures up to 330 °C using SYLTHERM 800. The measurement with water at low temperatures (20–50 °C) was performed in order to validate the high measurement accuracy of the flow through calorimeter. The calorimeter deviates less than 0.1% from the IAPWS (2007) denoted values.

From the comparison to a laboratory DSC results, it is concluded that the calorimeter bypass measures the heat capacity accurately at temperatures up to 270 °C (< 1.2% deviation to DSC); values see Table 3. Especially above this temperature, the readings of the Coriolis mass flow sensor seem not reliable anymore, because the temperature dependent uncertainty of the Coriolis mass flow sensor cannot be traced back to a valid calibration or examination at elevated temperatures. At a temperature of 330 °C, the measured heat capacity deviated 3.7% from the DSC results. To overcome this, it is planned to install an additional heat exchanger to maintain temperatures seen by the Coriolis sensor below 200 °C.

The specific heat capacity of the SYLTHERM 800 used at the KONTAS facility was quantified in order to enhance the accuracy of tests performed at this facility. Moreover, the functionality and limitations of the actual calorimeter bypass were demonstrated. The established measurement procedure revealed that the achievement of the required thermal equilibrium/ steady state conditions within the measurement bypass including its thermal insulation especially at temperatures above 300 °C takes several hours. Considering just the wetted steal parts, steady-state conditions are reached within 15 min especially for minor inlet temperature adjustments. The results of several heat loss measurements within the range of typical operation temperatures provide necessary heat loss data to be respected during heat capacity measurements.

It can be concluded, that for the actual status of the HTF of the KONTAS facility, the heat capacities provided by the HTF manufacturer should not be used for test evaluations. Instead, the mean value between the DSC laboratory measurements and the value measured by the flow through calorimeter is recommended, until the heat exchanger/ cooler for the Coriolis sensor is installed. Apart from the upgrade with the heat exchanger, it is planned to undertake further measurements at different facilities, also to examine aging processes of HTF. Additionally

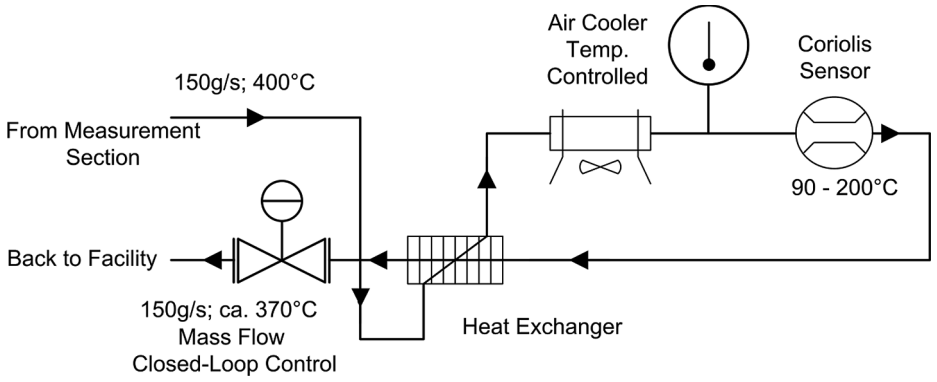

Fig. 14. Tubing diagram (draft) to operate the Coriolis mass flow sensor at temperatures below 200 °C while measuring cp values up to 400 °C.

to the heat capacity measurement, the bypass can be used to recalibrate installed mass flow sensors of these installations. This option is enabled by the mobility and stand-alone data acquisition system of the calorimeter.

Declaration of Competing Interest

The authors declare that they have no known competing financial interests or personal relationships that could have appeared to influence the work reported in this paper.

Acknowledgements

The authors would like to thank the Federal Ministry for the Environment, Nature Conservation, Building and Nuclear Safety for funding the “KONTAS-Pro” project (0325214) which included the primary setup and the cold commissioning and for funding the “QuarzZert” project (0325712) for heat capacity measurements at the KONTAS facility. Further improvements regarding measurement accuracy, the hot commissioning and first oil measurements were supported by the European Commission (FP7-INFRASTRUCTURES-2012-1) within the scope of the “SFERA II” project (312643).

References

ASTM International, 2011. E1269 - 11 International Standard Test Method for Determining Specific Heat Capacity by Differential Scanning Calorimetry.

Barroso, H., Sanz, F., Hernández, M., Pereira, D., Rayo, D., Serrano, E., 2012. Understanding of the HTF degradation on parabolic trough power plant energy performance. In: SolarPACES 2012.

Christensen, J.J., Brown, P.R., Izatt, R.M., 1986. An isothermal flow calorimeter for high temperature aqueous solutions. Thermochim. Acta 99, 159–168.

Collares-Pereira, M., Duque, J., Saraiva, C., Rego Teixeira, A., 1981. A calorimeter for solar thermal collector testing. Sol. Energy 27, 581–582.

Dauncey, M.J., Murgatroyd, P.R., Cole, T.J., 1978. A human calorimeter for the direct and indirect measurement of 24h energy expenditure. Br. J. Nutr. 39, 557.

DOW, 1997. SYLTHERM 800 Heat Transfer Fluid Product Technical Data: Dow Chemical Company.

Ernst, G., Maurer, G., Wiederuhb, E., 1989. Flow calorimeter for the accurate determination of the isobaric heat capacity at high pressures; results for carbon dioxide. J. Chem. Thermodyn. 21, 53–65.

Fernández-García, A., Cantos-Soto, M.E., Röger, M., Wieckert, C., Hutter, C., Martínez-Arcos, L., 2014. Durability of solar reflector materials for secondary concentrators used in CSP systems. Sol. Energy Mater. Sol. Cells 130, 51–63.

Gomez, J.C., Glatzmaier, G.C., Mehos, M., 2012. Heat Capacity uncertainty calculation for the eutectic mixture of biphenyl/diphenyl ether used as heat transfer fluid. In: SolarPACES 2012.

Handa, Y.P., 1986. Compositions, enthalpies of dissociation, and heat capacities in the range 85 to 270 K for clathrate hydrates of methane, ethane, and propane, and enthalpy of dissociation of isobutane hydrate, as determined by a heat-flow calorimeter. J. Chem. Thermodyn. 18, 915–921.

HELIOSCSP, Solar Thermal Energy News, PROTERMOSOLAR, 2019. Concentrated Solar Power increasing cumulative global capacity more than 11% to just under 5.5 GW in 2018, http://helioscsp.com, accessed October 10th 2019.

Heller, P., Meyer-Grünefeldt, M., Ebert, M., Janotte, N., Nouri, B., Pottler, K., Prahl, C., Reinalter, W., 2011. KONTAS - a rotary test bench for standardized qualification of parabolic trough components. SolarPACES Conference 2011.

Hilgert, C., Bern, G., Röger, M., 2012. Kontas-CP - flow through calorimeter for online heat capacity measurement of thermal oils in CSP application. In: SolarPACES 2012.

IAPWS, 2007. The International Association for the Properties of Water and Steam: Revised Release on the IAPWS Industrial Formulation 1997 for the Thermodynamic Properties of Water and Steam, http://www.iapws.org/relguide/IF97-Rev.pdf, accessed October 10th 2019.

JCGM, 2008. Joint Committee for Guides in Metrology: JCGM 100: Evaluation of Measurement Data - Guide to the Expression of Uncertainty in Measurement, 2008.

Jung, C., Nietsch, A., 2014. Precise Heat Capacity Determination of Organic Heat Transfer Fluids.

Marchã, J., Osório, T., Collares-Pereira, M., Hort, P., 2014. Development and test results of a calorimetric technique for solar thermal testing loops, enabling mass flow and Cp measurements independent from fluid properties of the HTF used. Energy Procedia 49, 2125–2134.

NREL, National Renewable Energy Laboratory, 2019. Concentrating Solar Power Projects, https://solarpaces.nrel.gov/, accessed October 10th 2019.

Muñoz-Sánchez, B., Nieto-Maestre, J., Gorka, I., Izaskun, M., Iñigo, I.-T., Ana, G.-R., et al., 2017. A precise method to measure the specific heat of solar salt-basednanofluids. J. Therm. Anal. Calorimetry 129, 905–914. https://doi.org/10.1007/s10973-017-6272-x.

Rudtsch, S., 2002. Uncertainty of heat capacity measurements with differential scanning calorimeters. Thermochim. Acta 382, 17–25.

Segovia, J.J., Vega-Maza, D., Chamorro, C.R., Martín, M.C., 2008. High-pressure isobaric heat capacities using a new flow calorimeter. J. Supercrit. Fluids 46, 258–264.

SETARAM, 2014. Technical Data Sheet, SENSYS TG-DSC: SETARAM Instrumentation, https://www.setaram.de/wp-content/uploads/2018/10/SENSYS-TG-DSCevo-EN.pdf accessed October 10th 2019.

Taberner A.J., Johnston C.M., Pham T., June-Chiew Han T., Ruddy B.P., Loiselle D.S., Nielsen P.M., 2015. Measuring the mechanical efficiency of a working cardiac muscle sample at body temperature using a flow-through calorimeter. In: Conf Proc IEEE Eng Med Biol Soc. 2015 Aug.